available at www.sciencedirect.com

SCIENCE DIRECT®

journal homepage: www.elsevier.com/locate/biochempharm

Stereospecific recognition of a spirosuccinimide type aldose reductase inhibitor (AS-3201) by plasma proteins: A significant role of specific binding by serum albumin in the improved potency and stability

Masuo Kurono *, *Akihito Fujii*, *Makoto Murata* [1], *Buichi Fujitani* [2], *Toshiyuki Negoro*

Chemistry Research Laboratories, Dainippon Pharmaceutical Co. Ltd., Enoki 33-94, Suita, Osaka 564-0053, Japan

ARTICLE INFO

Article history:
Received 9 August 2005
Accepted 20 October 2005

Keywords:
Human serum albumin
Aldose reductase inhibitor
Drug-binding site
Diabetic plasma
Stereospecificity
Binding mode

Abbreviations:
α_1-AGP, (human) α1-acid glycoprotein
AKR1B, aldose reductase
Compound 1 (racemate), 2-[(4*R*,*S*)-2-(4-bromo-2-fluorobenzyl)-1,3-dioxo-1,2,3,4-tetrahydropyrrolo[1,2-a]pyrazin-4-yl]acetamide
Compound 2 (racemate), (3*R*,*S*)-2′-(4-bromo-2-fluorobenzyl)spiro[pyrrolidine-3,4′(1′*H*)-6′-chloropyrrolo[1,2-*a*]pyrazine]-1′,2,3′,5(2′*H*)-tetrone

ABSTRACT

AS-3201 [(3*R*)-2′-(4-bromo-2-fluorobenzyl)spiro[pyrrolidine-3,4′(1′*H*)-pyrrolo[1,2-*a*]pyrazine]-1′,2,3′,5(2′*H*)-tetrone] is a structurally novel and stereospecifically potent aldose reductase (AKR1B; EC 1.1.1.21) inhibitor, which contains a succinimide ring that undergoes ring-opening at physiological pH levels. To delineate intermolecular interactions governing its favorable pharmacokinetic profile, the interaction of AS-3201 (*R*-isomer) with plasma proteins, especially human serum albumin (HSA), was examined in comparison with that of the optical antipode (*S*-isomer). Fluorescence, kinetic, and high-performance frontal analyses showed that the *R*-isomer is more strongly bound than the *S*-isomer to sites I and II on HSA, and the *R*-isomer is particularly protected from hydrolysis, suggesting that the stable HSA–*R*-isomer complex contributes to its prolonged activity. The thermodynamic parameters for the specific binding indicated that in addition to hydrophobic interactions, hydrogen bonds contribute significantly to the *R*-isomer complex formation. ^{13}C NMR observations of the succinimide ring (5-^{13}C enriched), which are sensitive to its ionization state, suggested the presence of a hydrogen bond between the *R*-isomer and HSA, and ^{19}F NMR of the pendent benzyl ring (2-^{19}F) evaluated the equilibrium exchange dynamics between the specific sites. Furthermore, fatty acid binding or glycation (both are site II-oriented perturbations) inhibited the binding to one of the specific sites and reduced the stereospecificity of HSA toward the isomers, although the clinical influence of these perturbations on the *R*-isomer binding ratio seemed to be minor. Thus, the difference in the interaction mode at site II might be a major cause of the stereospecificity; this is discussed on the basis of putative binding modes. The present results, together with preliminary absorption and distribution profiles, provide valuable information on the stereospecific pharmacokinetic and pharmacodynamic properties of the *R*-isomer relevant for the therapeutic treatment of diabetic complications.

* *Corresponding author*. Tel.: +81 6 6337 5886; fax: +81 6 6338 6010.
E-mail address: masuo-kurono@ds-pharma.co.jp (M. Kurono).

[1] Present address: Research Management, Dainippon Pharmaceutical Co. Ltd., Enoki 33-94, Suita, Osaka 564-0053, Japan.

[2] Present address: International Affairs, Dainippon Pharmaceutical Co. Ltd., Dosho-machi 2-6-8, Chuo-ku, Osaka 541-0045, Japan.

0006-2952/$ – see front matter © 2005 Elsevier Inc. All rights reserved.
doi:10.1016/j.bcp.2005.10.036

DNSA, 5-dimethylaminonaphthalene-1-sulfonamide
DSP, diabetic sensorimotor polyneuropathy
FA-HSA, fatty acid containing HSA
G-HSA, glycated HSA
HSA, fatty acid-free human serum albumin
HPFA, high-performance frontal analysis
PA, palmitic acid
R-isomer (AS-3201), (3R)-2′-(4-bromo-2-fluorobenzyl)spiro[pyrrolidine-3,4′(1′H)-pyrrolo[1,2-a]pyrazine]-1′,2,3′,5(2′H)-tetrone
RSA, fatty acid-free rat serum albumin
SDS, sodium dodecyl sulfate
S-isomer, (3S)-2′-(4-bromo-2-fluorobenzyl)spiro[pyrrolidine-3,4′(1′H)-pyrrolo[1,2-a]pyrazine]-1′,2,3′,5(2′H)-tetrone

1. Introduction

Various biological phenomena are ascribable to the binding of specific ligands to enzymes, receptors and biomembranes. Examining the nature of such interactions is, therefore, of great interest in understanding any given biological process and in developing more effective drugs. Plasma proteins are responsible for transportation of many ligand molecules and for the regulation of colloid osmotic pressure in blood vessels, while drug–plasma protein binding is an important process in determining the activity and fate of a drug once it has entered the body. Since free (i.e., protein unbound) drugs can easily permeate through capillary vessels and glomerular membranes in the nephrons, their distribution and elimination are often correlated with free drug fraction, and sometimes with competition for binding sites on plasma proteins. Indeed, the degree of plasma protein binding affects clearance and lifetime profile of drugs in vivo, and microenvironmental changes such as non-enzymatic glycation and elevated fatty acids in diabetic plasma can influence the binding of certain drugs and their pharmacokinetics [1–5]. Thus, aside from enzymes, receptors and biomembrane, plasma proteins are additional important targets for drug development. Clear and quantitative information on the nature of a given drug–plasma protein interaction should provide a firm basis for its rational use in clinical practice.

(3R)-2′-(4-bromo-2-fluorobenzyl)spiro[pyrrolidine-3,4′(1′H)-pyrrolo[1,2-a]pyrazine]-1′,2,3′,5(2′H)-tetrone (AS-3201, Fig. 1), is a structurally novel, and stereospecifically potent inhibitor of aldose reductase (AKR1B; EC 1.1.1.21) with improved pharmacokinetics [6]. Since AKR1B catalyzes the NADPH-dependent reduction of glucose to sorbitol, a membrane impermeable polyol that accumulates in cell, a control of AKR1B activity is necessary to delay or prevent secondary diabetic complications and biochemical changes associated with hyperglycaemia [7]. AS-3201 (R-isomer) is more potent in both in vitro and in vivo activities than its optical antipode (S-isomer, Fig. 1), and shown to have beneficial effects on diabetic sensorimotor polyneuropathy (DSP) in patients [8]. Our previous study on the interaction of these compounds with its target enzyme AKR1B revealed that the difference in stereostructure in the spirosuccinimide moiety not only causes a substantial change in the inhibitor constant but also induces differentiation between AKR1B and aldehyde reductase (a closely related enzyme) [9]. However, although both isomers undergo ring-opening at physiological pH levels, as is

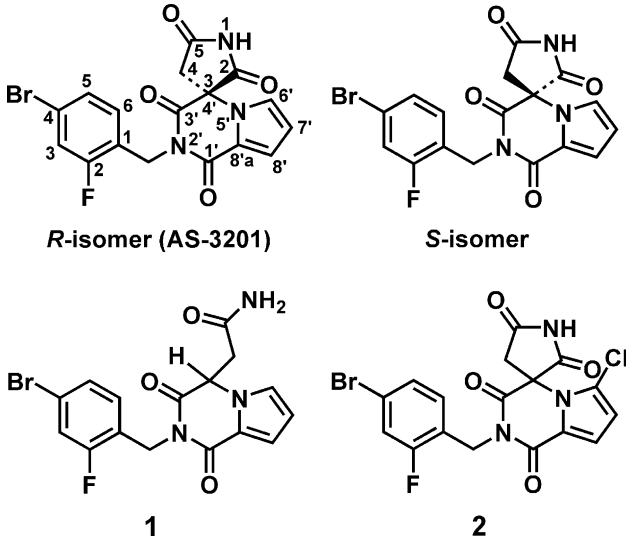

Fig. 1 – Chemical structures of the R-isomer (AS-3201) and related compounds. The asymmetric carbon that determines the R- or S-configuration is C3 (C4′) of the molecule.

the case with succinimide [10], and yield an inactive compound 1 (racemate, Fig. 1), intermolecular interactions governing the prolonged AKR1B inhibitory activity of the *R*-isomer in vivo are not yet fully understood. In this study, we have quantitatively characterized the binding of the *R*-isomer to plasma proteins, especially human serum albumin (HSA). In common with serum albumins from other species, HSA is the most abundant protein in blood plasma, present at ~600 μM, and serves as the primary transport protein for many metabolites, fatty acids and lipophilic drugs possessing acidic or electronegative functional groups [5,11]. X-ray structural studies have revealed the location of the fatty acid binding sites distributed throughout the protein [12,13] and have assigned the position of two primary drug-binding sites, known as sites I and II [14] to subdomains IIA and IIIA [15]. However, great difficulty may be experienced in investigating the ligand binding properties of HSA, because of the diversity of acceptable ligands, the ability to bind more than one ligand at the same time, and the potential for allosteric interactions between ligand-binding sites [5,11]. To accomplish our objective, the *R*-isomer and its optical antipode (*S*-isomer) have been studied as ligands of HSA using fluorometric titration, hydrolysis kinetics, high-performance frontal analysis (HPFA), and NMR spectroscopy in a concerted fashion. In particular, the observation of the NMR signals from the succinimide ring (5-^{13}C enriched) and the pendent benzyl ring (2-^{19}F) of the isomers is useful for direct examination of their ionization behavior, the filling of individual binding sites on HSA and the exchange dynamics between these sites. The comparative analyses of the binding characteristics of these isomers to HSA enabled us to investigate the biophysical factors underlying the stereospecifically improved stability and potency of the *R*-isomer; these factors will help to address questions about its pharmacological and potential clinical significance.

2. Materials and methods

2.1. Materials

Fatty acid-free (<0.005%) and globulin-free HSA (HSA, Ca. No. A-3782; lot 32H9300), fatty acid containing HSA (FA-HSA, Ca. No. A-8763; lot 105H9308), glycated HSA (G-HSA, Ca. No. A-8301; lot 094H8270, 3.0 mol hexose per mole albumin), human α_1-acid glycoprotein (α_1-AGP, Ca. No. G-9885; lot 90H9317), and fatty acid-free (<0.005%) rat serum albumin (RSA, Ca. No. A-2018; lot 51H9305) were purchased from Sigma Chemical Co. (St. Louis, MO, USA). Although HSA typically carries 1–2 fatty acids molecules under physiological conditions [5], commercial preparations of fraction V powder usually have a high content of fatty acids (5–10 mol of fatty acid/mol albumin) [16]. Therefore, it is essential to consider fatty acid content of commercial HSA preparations when comparing studies of drug binding to HSA. The fatty acid contents of HSA, FA-HSA, G-HSA, and RSA were determined according to the method previously described [17] and found to be <0.01, 8.1, 4.0, and <0.01 mol fatty acids per mole albumin, respectively. All these proteins were reconstituted in 1/15 M phosphate buffer (pH 7.4, ionic strength 0.17). *R*-isomer (optical purity ≥ 99.8% e.e.), *S*-isomer (optical purity ≥ 99.8% e.e.), a succinimide ring-opened compound 1 (racemate), and compound 2 (internal standard, I.S., racemate) (Fig. 1) were synthesized according to the procedures previously described [6]. The compounds were dissolved in a mixture of 1 mM citric acid (pH 2.8)–acetonitrile (90/10, v/v) to desired concentrations before use. This solvent prevented the hydrolysis of these compounds, and had no influence on the binding properties of the *R*- and *S*-isomers [9]. [1-^{13}C]ethyl bromoacetate (98% ^{13}C-enriched) was obtained from Aldrich Chemical Co. (Milwaukee, WI, USA). Fluorescent probes, 5-dimethylaminonaphthalene-1-sulfonamide (DNSA), warfarin, dansylsarcosine, and dansyl-L-proline [14,18] were also from Sigma. All other reagents used in the present study were analytical grade and used without further purification. Distilled and deionized (<0.1 μS/cm) water was used for all the measurements.

2.2. Synthesis of the [5-^{13}C] isomers

[5-^{13}C] *R*-isomer and [5-^{13}C] *S*-isomer were prepared and characterized according to the method previously described [6]. In the initial step, ethyl benzyloxycarbonylaminocyanoacetate (13.1 g) was alkylated with [1-^{13}C]ethyl bromoacetate (7.0 g) instead of the unlabeled ethyl bromoacetate. The remainder of the synthesis procedures was then accomplished in exactly the same manner. Finally, the [5-^{13}C] *R*-isomer (0.2 g, 6.4%, 99.6% e.e.) and the [5-^{13}C] *S*-isomer (0.4 g, 5.1%, 99.9% e.e.) were obtained and their physical properties were confirmed by ^{1}H NMR, IR, and mass spectra as well as elemental analyses: ^{1}H NMR (DMSO-d_6) δ 3.56 (2H, s), 5.00 (2H, m), 6.52 (1H, dd, J = 4.0, 2.8 Hz), 7.12 (1H, dd, J = 3.8, 1.4 Hz), 7.14 (1H, t, J = 8.2 Hz), 7.36 (1H, dd, J = 8.4, 2.0 Hz), 7.54 (1H, dd, J = 9.8, 2.0 Hz), 7.72 (1H, dd, J = 2.6, 1.6 Hz), and 12.16 (1H, s); IR (KBr, cm^{-1}) 3130 (NH), 1785 (CO), 1710 (CO), and 1670 (CO); MS (m/z) 421 (MH^+). Anal. Calcd for $^{12}C_{16}{}^{13}CH_{11}BrFN_3O_4$: C, 45.63; C^{13}, 3.09; H, 2.63; N, 9.98; Br, 18.97; F, 4.51. Found for the [5-^{13}C] *R*-isomer: ^{12}C, 45.69; C^{13}, 3.09; H, 2.55; N, 9.99; Br, 18.75; F, 4.47. Found for the [5-^{13}C] *S*-isomer: ^{12}C, 45.63; C^{13}, 3.09; H, 2.61; N, 9.94; Br, 19.04; F, 4.63. The optical purity of the isomers was determined by HPLC analysis on an ULTRON ES-OVM chiral column (15 cm × 60 mm i.d., Shinwa Chemical Industries, Ltd., Kyoto, Japan) with mobile phase composed of 20 mM potassium dihydrogen phosphate–acetonitrile (80/20, v/v) at a flow rate of 1 mL/min. The column temperature was maintained at 25 °C and the eluent was monitored at 230 or 261 nm. The carbon-13 contents of the [5-^{13}C] isomers were confirmed to be ≥98% by mass spectrometry.

2.3. Examination of isomers binding by means of fluorescence quenching

Fluorescence measurements were made at 25 °C with an RF-5300 spectrofluorophotometer (Shimadzu, Kyoto, Japan) with a thermostated, magnetically stirred cell compartment. Titrations were carried out by serial addition of aliquots (3–5 μL) of ligand solutions to 3 mL of 0.5 μM plasma protein (HSA or α_1-AGP) solution, with excitation and emission wavelengths set at 280 and 340 nm (5 nm bandwidth), respectively. The fluorescence intensities were typically obtained 2 min after addition of ligand, and the data were corrected for background

Raman scattering, dilution effects and inner filter effects as reported previously [19]. In most cases, except for the HSA–*R*-isomer interaction, the fluorescence intensity decreases at ligand concentrations much greater than the protein concentration ($L_t \gg P_t$), and the data were fitted to Eq. (1),

$$\Delta F = \frac{\Delta F_{max} L_f}{(K_{dFL} + L_f)} \quad (1)$$

where ΔF is the fluorescence intensity decrease relative to the fluorescence intensity of the free protein, ΔF_{max} the maximum fluorescence decrease, K_{dFL} is the dissociation constant obtained by fluorescence quenching. L_f is the free ligand concentration and can be approximated by the total ligand concentration L_t under these conditions. On the other hand, since the *R*-isomer is an effective ligand at concentrations similar to that of the plasma protein, allowance must be made for the reduction in the concentration of the free *R*-isomer, and binding parameters were determined using the following equation (Eq. (2)), assuming the equivalence and independence of the binding sites [20],

$$\Delta F = \frac{\Delta F_{max}}{2nP_t} \times \left\{ (nP_t + L_t + K_{dFL}) - \sqrt{(nP_t + L_t + K_{dFL})^2 - 4nP_tL_t} \right\} \quad (2)$$

where n is the number of binding sites per mole protein and P_t is the total protein concentration. When the value of L_t is much greater than P_t ($L_t \gg nP_t$), Eq. (2) becomes identical to Eq. (1). The parameters, ΔF_{max} and K_{dFL} (and n) were estimated from the dependence of ΔF on L_t, and values of K_{dFL} were extracted. When the ligand binds to more than one binding site, the K_{dFL} value is the average dissociation constant since the fluorescence analysis does not distinguish between these interactions.

2.4. Displacement of fluorescent probe

To determine the isomers binding sites on HSA, competitive binding experiments were performed with a 10 μM HSA solution using fluorescent probes specific for sites I and II (site I: DNSA; site II: dansylsarcosine and dansyl-L-proline) [14,18]. The probe/HSA ratio was kept 1/5 in order to avoid non-specific binding, and the binding of the isomers were investigated by monitoring fluorescence quenching of the HSA–probe complex, with excitation and emission wavelengths set at 350 and 480 nm, respectively.

2.5. Retardation of the isomers hydrolysis by serum albumin

The hydrolysis reactions were initiated at pH 7.4 and 25 °C by adding the *R*- or *S*-isomer to the buffer or buffered albumin solution. To keep the non-specific interaction between the isomers and albumin to a minimum, the final concentration of the isomers was kept more than six-fold lower than that of the albumin. At appropriate intervals, aliquots of the reaction mixture were directly injected onto a NOVA PAK C18 column (4 μm, 30 cm × 3.9 mm i.d., Waters, Milford, MA, USA) with mobile phase composed of 40 mM phosphate (pH 3.0)–acetonitrile (50/50, v/v) containing 5 mM SDS at a flow-rate of 1 mL/min. The residual concentration was determined from the peak area at 296 nm and apparent hydrolysis rate constants (k_{app}) were estimated by fitting the time–residual concentration data to an exponential decay curve. When the hydrolysis proceeds through the pathway shown in Scheme 1, the k_{app} values obtained at different concentrations of albumin can be represented by Eq. (3) as described previously [21].

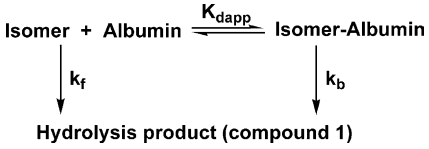

Scheme 1 – Hydrolysis pathway of the isomer in the presence of albumin. K_{dapp} is the apparent dissociation constant for the specific interaction with albumin, k_f and k_b are hydrolysis rate constants of free and bound isomer, respectively.

$$k_{app} = \frac{(k_f K_{dapp} + k_b P_f)}{(K_{dapp} + P_f)} \quad (3)$$

where K_{dapp} is the apparent dissociation constant for the specific interaction with albumin, k_f and k_b are hydrolysis rate constants of free and bound isomer, respectively. P_f is the concentration of free albumin and can be approximated by its total concentration P_t, because the concentration of albumin was much larger than that of the isomer under the present conditions. When the isomers bind to albumin at n independent and equivalent binding sites, K_{dapp} denotes K_d/n (K_d and n are the dissociation constant and the number of binding sites, respectively) and k_b can be expressed as the average value of the hydrolysis rate constants for the *R*- or *S*-isomer bound to respective binding sites on albumin.

2.6. Determination of the free isomer concentration by means of HPFA

The free isomer concentration was measured by means of HPFA [22,23]. Since HPFA is a simple and less time-consuming chromatographic method, the obtained data are almost uninfluenced by the hydrolysis of the isomers. In addition, this method does not suffer from undesirable drug adsorption on membrane nor leakage of bound drug through the membrane often encountered in conventional equilibrium dialysis or ultrafiltration, and therefore, is useful for accurate analysis of strongly bound drugs.

In brief, the HPFA method involved the direct injection of an HSA–isomer mixed solution (0.25–1.3 mL) onto an internal-surface reversed-phase silica column (5 μm, 5 cm × 4.6 mm i.d., Regis Chemical Co., Morton Grove, IL, USA) [24], which was equilibrated with phosphate buffer (pH 7.4, ionic strength 0.17) at a flow-rate of 1 mL/min. When the injection volume was sufficient, the binding equilibrium in the sample solution was reproduced in the column, and the free isomer was eluted as a trapezoidal peak with a plateau region on the chromatogram after the firstly-eluted protein peak. Thus, following the direct injection of a sample, the free isomer concentration in the initial sample solution was determined from the plateau

height with detection at 296 nm. The column and the mobile phase temperatures were maintained at the desired temperatures. The binding parameters were determined according to the Langmuir isotherm model (Eq. (4)):

$$B = \frac{L_b}{P_t} = \sum_{i=1}^{z} \frac{n_i L_f}{K_{di} + L_f} + \frac{L_f}{(K_d/n)'} \quad (4)$$

where B is the bound isomer concentration per mole albumin, L_b the bound isomer concentration, P_t the total albumin concentration, z the number of specific binding classes, n_i and K_{di} are, respectively, the number of binding sites and the dissociation constant for the ith class, L_f the free isomer concentration, and $(K_d/n)'$ represents the non-specific binding component. By varying the values of z (i.e., z = 1, 2 or 3), the most appropriate model with or without non-specific binding $(K_d/n)'$ was chosen on the basis of reduced chi-square (chi-square divided by the degree of freedom) [25] and standard errors of estimates (<25% of the values) [26]. To achieve saturation of the binding capacity of HSA, the experiments were carried out at HSA concentrations (70–140 μM) less than found under physiological conditions (~600 μM). In this concentration range, experiments gave points located on the same curves, as expected if HSA is monomeric and HSA-to-HSA interaction is negligible.

The thermodynamic parameters for the specific binding of the *R*- and *S*-isomers to HSA were determined from the temperature dependence of the binding parameters between 15–37 °C. Since the van't Hoff plots ($-\ln K_{d1}/n_1$ versus $1/T$) for the specific binding were essentially linear (see Section 3), the standard Gibbs energy change (ΔG°), the enthalpy change (ΔH°), and the standard entropy change (ΔS°) were calculated according to Eq. (5).

$$\Delta G^\circ = -RT\ln\left(\frac{K_{d1}}{n_1}\right) = \Delta H^\circ - T\Delta S^\circ \quad \text{or}$$
$$-\ln\left(\frac{K_{d1}}{n_1}\right) = -\frac{\Delta H^\circ}{R}\left(\frac{1}{T}\right) + \frac{\Delta S^\circ}{R} \quad (5)$$

2.7. Protein concentration

Protein concentrations were measured on a weight-to-volume basis, and the molecular weights of albumins and α_1-AGP were assumed to be 66000 [27] and 44100 [28], respectively. Occasionally, HSA concentrations were determined spectrophotometrically using $E^{1\,cm,\,1\%}_{280\,nm}$ = 5.3 [29]. The HSA concentrations obtained by the latter method agreed very closely with those obtained by the former.

2.8. NMR spectral measurements

Samples containing HSA (1.2 mM) with or without the [5-^{13}C] isomers were dissolved in 1/15 M phosphate buffer (pH 7.4). ^{13}C NMR spectra at 125.7 MHz and ^{19}F NMR spectra at 470.3 MHz were obtained on a Varian Unity-INOVA 500 spectrometer (Varian Associates, Palo Alto, CA, USA) equipped with a Sun SPARC workstation. ^{13}C NMR spectra were recorded using a 5-mm switchable probe, and broad-band proton decoupling was applied. The standard spectral parameters were as follows: 28 kHz spectral width; 39 K data points; 90° (10.1 μs) pulse width; 0.8 s acquisition time; 3.2 s relaxation delay; 10 Hz line broadening; 30,000–50,000 transients. Chemical shifts were measured with respect to TSP, and the nitrile signal of a trace of acetonitrile was used as a secondary reference (121.9 ppm). The pH dependence of the chemical shift resonance of the [5-^{13}C] isomers was examined in 1/15 M phosphate buffer. When lowering the pH below 4.5, the buffer was adjusted with phosphoric acid so as to obtain the appropriate pH. The apparent pK value was determined by fitting the data to Eq. (6),

$$\delta_{obs} = \frac{\delta_{low}10^{-pH} + \delta_{high}10^{-pK}}{10^{-pH} + 10^{-pK}} \quad (6)$$

where δ_{low} and δ_{high} are the limiting chemical shift resonances for the deprotonated and protonated [5-^{13}C] isomer.

^{19}F NMR spectra were observed using a 5-mm indirect detection probe without proton decoupling. The standard spectral parameters were as follows: 27 kHz spectral width; 65 K data points; 90° (14.5 μs) pulse width; 1.2 s acquisition time; 2.8 s relaxation delay; 3 Hz line broadening; 4000–6000 transients. Fluorine chemical shifts were measured with respect to $CFCl_3$, and a trace of trifluoroethanol was used as a secondary reference (−77.23 ppm).

2.9. Fitting of experimental data

Each parameter was calculated by fitting the experimental data to the appropriate Eqs. (1)–(6) using the Marquardt–Levenberg algorithm in Origin 6.0 (MicroCal Software, Northampton, MA, USA). A statistical weighting factor of $1/B$ was applied in the fitting to Eq. (4), while in re-fitting the calculated k_{app} and K_{d1}/n_1 values to Eqs. (3) and (5), respectively, the reciprocal of squared standard error was applied as weighting. The curves were drawn using the parameter values obtained by the fitting procedure.

2.10. Determination of the isomers in rat plasma and tissues by means of reversed-phase HPLC

Male Wistar rats weighting about 200 g were orally administered the separate isomers as a suspension in 0.5% (w/v) aqueous tragacanth solution. The collected biological samples were treated in the following way.

2.10.1. Plasma samples

The mixture of 0.5 mL of plasma spiked with 0.1 μg compound 2 (I.S.) and 0.5 mL of 0.2 M hydrochloric acid was extracted with 6 mL of dichloromethane. The organic layer (5 mL) was evaporated to dryness under a stream of nitrogen at room temperature. The residue was dissolved in 60 μL of acetonitrile and an aliquot of 20 μL was injected onto the column. The chromatographic conditions were the same as in Section 2.5 except that SDS was not employed in the current determinations.

2.10.2. Tissue homogenate samples

Lens, scitic nerve and kidney are target tissues of, respectively, cataract, neuropathy and nephropathy, and the target enzyme AKR1B mRNA was highly expressed in such target tissues of complications in rat [7]. These target tissues were homogenated in 5 mM phosphate buffer (pH 5.1) containing 0.9% (w/

Table 1 – Dissociation constants and hydrolysis rate constants for the isomers in the presence of plasma proteins at pH 7.4 and 25 °C[a]

Ligand	Fluorescence analysis		Kinetic (hydrolysis) analysis					
	HSA	α_1-AGP	HSA			RSA		
	K_{dFL} (μM)	K_{dFL} (μM)	K_{dapp}[b] (μM)	$k_b \times 10^3$ (h^{-1})	$k_f \times 10$ (h^{-1})	K_{dapp} (μM)	$k_b \times 10^4$ (h^{-1})	$k_f \times 10$ (h^{-1})
R-isomer	1.7 ± 0.2	12.1 ± 0.2	1.07 ± 0.07	2.6 ± 0.4	1.09 ± 0.04	0.16 ± 0.02	5.6 ± 1.0	1.0 ± 0.1
S-isomer	7.1 ± 0.6	16.5 ± 0.9	4.67 ± 0.25	4.4 ± 0.2	1.10 ± 0.04	0.41 ± 0.05	4.0 ± 0.5	1.0 ± 0.1

[a] The errors are the calculated standard errors of the fit.
[b] Since the R- or S-isomer binds to two binding sites (sites I and II) on HSA with similar affinities (see text), the K_{dapp} value corresponds to half the dissociation constant ($K_d/2$) and the k_b value to the average value of the hydrolysis rate constants for the isomer bound to sites I and II ($(k_{bI} + k_{bII})/2$).

v) sodium chloride and made up to 2–10% (w/v) supernatants of these homogenates at 0 °C followed by centrifugation at 1500 × *g* for 5 min. The mixture of 1 mL of the supernatant spiked with 0.1 μg I.S. and 0.2 mL of 0.2M hydrochloric acid was extracted with 6 mL of dichloromethane. The remainder of the procedure is the same as that described for plasma samples above.

3. Results

3.1. Fluorescence analysis of the R- and S-isomers binding to plasma proteins

As a preliminary step, the influence of the R- and S-isomers binding on the fluorescence of HSA and α_1-AGP, i.e., the main binding proteins in human plasma, was investigated. Both isomers acted as quenchers. Fig. 2 shows the dependence of fluorescence intensity of HSA at 340 nm (ΔF) on total concentration of the R- or S-isomer. The fluorescence intensity was largely decreased by the addition of the isomers, from which both isomers were clearly bound to this plasma protein. The dissociation constants (K_{dFL}) were estimated as described in Section 2 and are provided in Table 1, together with those for α_1-AGP. The affinities of the isomers for HSA were significantly higher than those for α_1-AGP. More remarkable is the fact that a distinct (4.2-fold) difference in the K_{dFL} values for HSA was observed between these two isomers. On the other hand, compound 1, which does not contain a succinimide, had significantly lower affinity for HSA than did both isomers (K_{dFL} = 25.2 ± 2.4 μM).

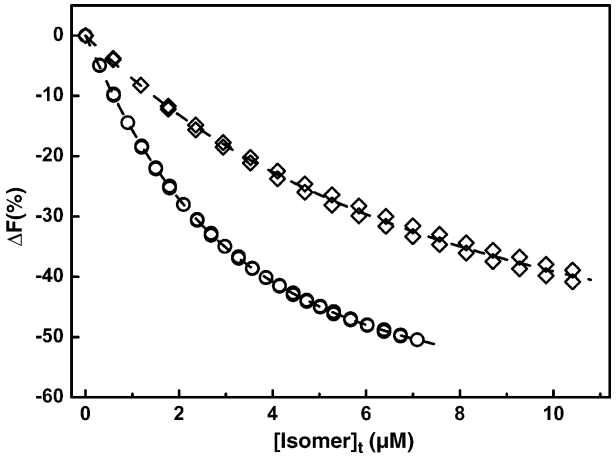

Fig. 2 – Dependence of the fluorescence intensity decrease of HSA at 340 nm on total concentration of the R-isomer (○) and the S-isomer (◇) at pH 7.4 and 25 °C.

3.2. Effect of the isomers on fluorescent probe bound to HSA

To gain information about the location of the isomers binding sites on HSA, fluorescent probe displacement was examined. Fluorescence intensity changes, upon dissociation from HSA by competition with ligands for binding sites, have been well characterized [14,18,30]. Fig. 3(a) shows the effects of the isomers and warfarin (site I binding drug) on the fluorescence of site I probe DNSA bound to HSA. The addition of either the isomers or warfarin decreased the fluorescence of the HSA–DNSA complex, corresponding to the dissociation of DNSA from its binding site (i.e., site I). The R-isomer displaced DNSA to a greater extent than did the S-isomer, in agreement with the greater binding affinity of the R-isomer for HSA. On the other hand, both isomers also displaced site II probe dansylsarcosine, whereas warfarin did not displace this site II probe (Fig. 3(b)). Similar results were obtained with another site II probe, dansyl-L-proline (data not shown). These results indicated that the isomers inhibit these probes binding to sites I and II on HSA.

3.3. Effect of serum albumin on the hydrolysis of the isomers

The isomers are somewhat unstable in aqueous solution at physiological pH so as to form compound 1[1] Since compound 1 does not contain the negatively charged (succinimide ring) moiety, which would tightly interact with the side chains of the active site residues of AKR1B [9], this compound has no

[1] In the hydrolysis, although the succinimide of the isomers can be ring-opened, probably by the nucleophilic attack of a water molecule or hydroxide ion at the 2-carbonyl position, the subsequent decarboxylation to form compound 1 (racemate) makes ring reclosure process (i.e., chiral inversion or racemization in the spirosuccinimide moiety) impossible. This is contrary to a previous report of rapid and complete racemization of other supirosuccinimide type ARIs [31] or thalidomide [32]. Details of such kinetics and mechanism of degradation will be published separately.

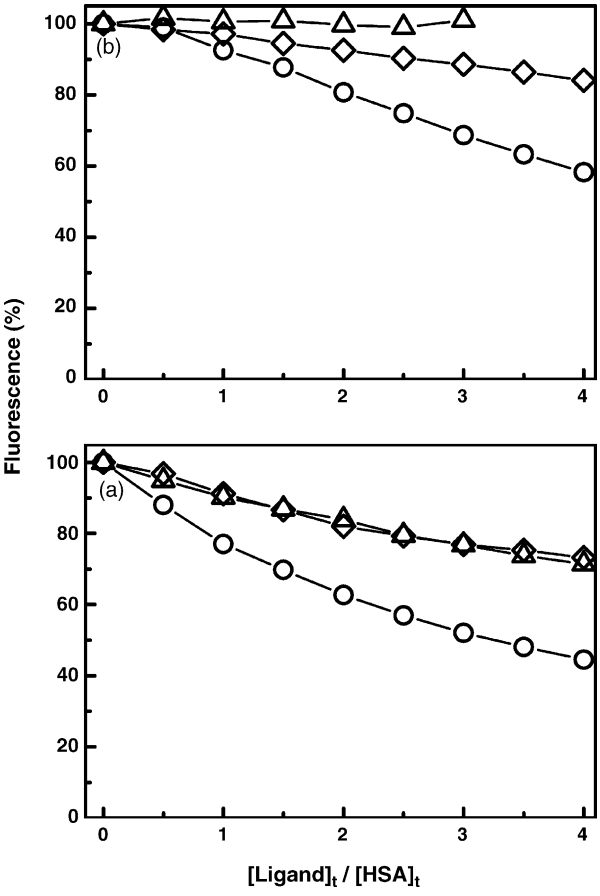

Fig. 3 – Displacement of fluorescent probes specific for HSA sites I and II, respectively, DNSA (a) and dansylsarcosine (b) by the *R*-isomer (○), the *S*-isomer (◇), and warfarin (△), plotted vs. the ligand/HSA ratio. HSA: 10 μM; probe: 2 μM.

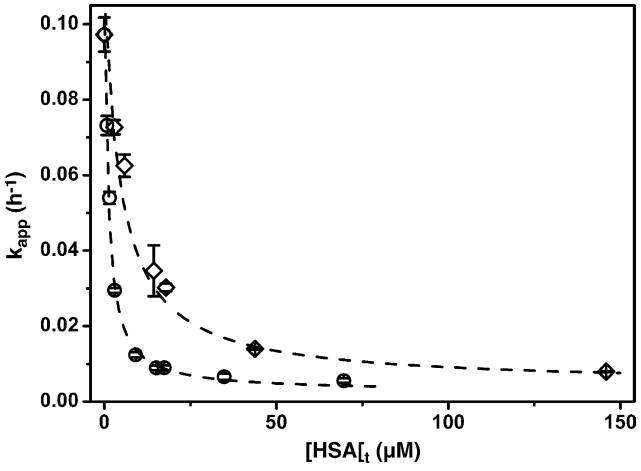

Fig. 4 – Effect of HSA concentration on the hydrolysis of the *R*-isomer (○) and the *S*-isomer (◇) at pH 7.4 and 25 °C.

inhibitory activity against the enzyme. To examine the in vitro hydrolysis of the isomers in HSA solution, the apparent hydrolysis rate constant (k_{app}) was determined from the time–residual concentration data for the isomers (see Section 2). As shown in Fig. 4, the k_{app} values of the isomers were quite similar in the absence of HSA and decreased as the concentration of HSA increased. These findings indicated that the binding to HSA is one of their stabilization mechanisms. The apparent dissociation constant of the *R*- or *S*-isomer from HSA (K_{dapp}), and the hydrolysis rate constants of its free and bound forms (k_f and k_b) were estimated by fitting these kinetic behaviors to Eq. (3) (Table 1). The bound *R*-isomer decomposed 42-fold slower than the free *R*-isomer, while 1.7-fold slower than the bound *S*-isomer. The latter indicates the relative inaccessibility of the bulk solvent to the succinimide ring of the *R*-isomer in the complex with HSA. The effect of serum albumin from rat (RSA) on the hydrolysis of the isomers was also examined (Table 1). RSA was found to bind and stabilize the isomers more significantly than HSA, and stereospecificity was also observed, with the *R*-isomer being 2.6-fold stronger than the *S*-isomer. The K_{dapp} values were in the sub-μM range, and the k_b value of the *R*-isomer was 180-fold smaller than its k_f value.

3.4. *Investigation of the isomers specific and non-specific bindings to HSA by means of HPFA*

To further investigate the specific and non-specific binding characteristics of the isomers to HSA, the mixed solutions of the *R*- or *S*-isomer and HSA were subjected to HPFA (see Section 2). Fig. 5(a) depicts the Langmuir plots for the isomers binding to HSA. It is noteworthy that the stereospecific interaction with HSA was dependent on the isomer concentration. The *R*-isomer was more bound than the *S*-isomer at lower concentrations, and less bound at higher concentrations. Under these HPFA conditions, saturation of the binding sites was not attained even at the highest concentration of the isomers testable (~0.4 mM). The binding data were best fit to a model consisting of one class of specific binding sites with non-specific binding (Eq. (4), z = 1) and the calculated binding

Table 2 – Binding parameters for the specific and non-specific binding of the isomers to HSA, FA-HSA and G-HSA obtained by HPFA at pH 7.4 and 25 °C

Ligand	HSA			FA-HSA			G-HSA		
	n_1[a]	K_{d1} (μM)	$(K_d/n)'$ (μM)	n_1	K_{d1} (μM)	$(K_d/n)'$ (μM)	n_1	K_{d1} (μM)	$(K_d/n)'$ (μM)
R-isomer	2.22 ± 0.08	1.61 ± 0.10	36.3 ± 2.7	0.86 ± 0.05	6.01 ± 0.53	52.8 ± 1.7	1.17 ± 0.04	4.00 ± 0.21	34.6 ± 0.9
S-isomer	1.95 ± 0.19	7.32 ± 1.00	24.5 ± 1.8	1.38 ± 0.06	17.4 ± 0.9	53.8 ± 1.6	1.50 ± 0.09	8.75 ± 0.69	33.1 ± 1.5

[a] n_1 is the number of specific binding site per albumin molecule, K_{d1} is the dissociation constant for the specific interaction, and $(K_d/n)'$ is the non-specific binding component.

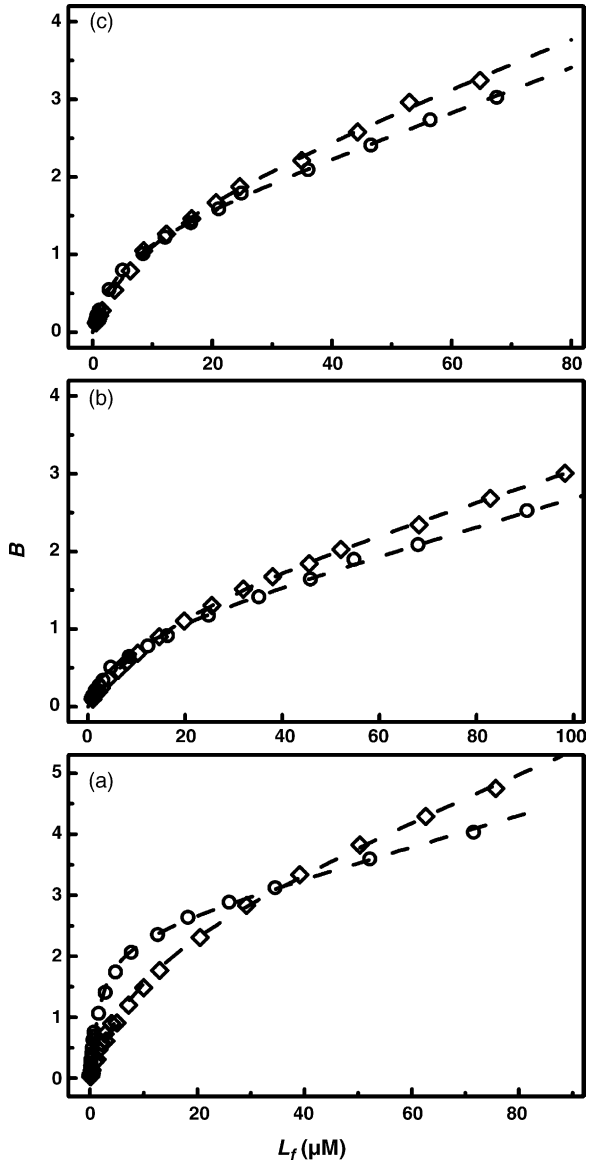

Fig. 5 – Binding of the *R*-isomer (○) and the *S*-isomer (◇) to HSA (a), FA-HSA (b) and G-HSA (c) at pH 7.4 and 25 °C. B: [bound isomer]/$[HSA]_t$, and $[L]_f$: the free concentration of the *R*- or *S*-isomer.

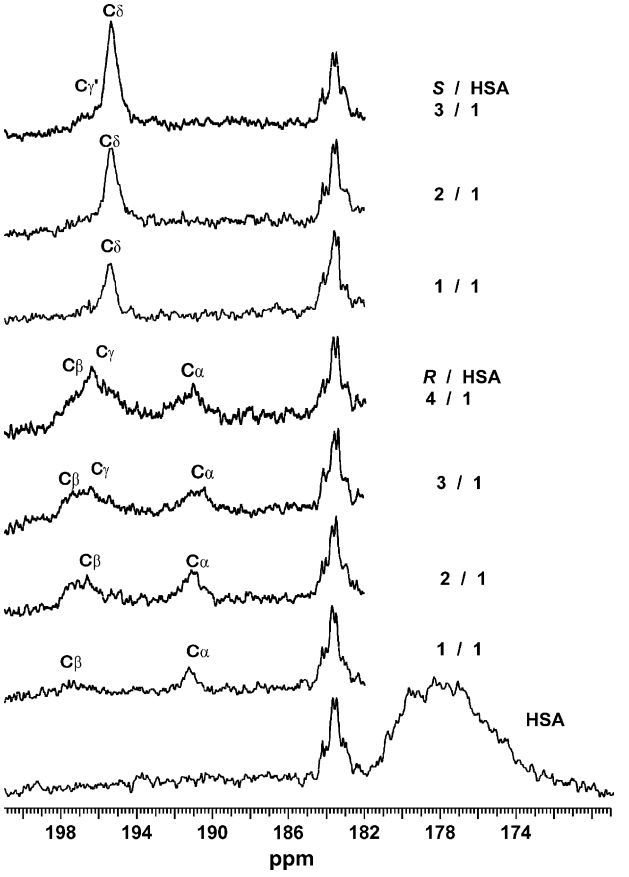

Fig. 6 – ^{13}C NMR spectra (carboxyl/carbonyl region) of the [5-^{13}C] *R*- or *S*-isomer at different the isomer/HSA mole ratios at pH 7.4 and 25 °C. HSA: 1.2 mM. *R*: *R*-isomer and *S*: *S*-isomer.

parameters are shown in Table 2. Both isomers are bound to a similar number of specific binding sites (i.e., two sites) on the HSA molecule. However, the *R*-isomer displayed about 5-fold higher affinity for the specific binding (K_{d1}/n_1) and 1.5-fold lower affinity for the non-specific binding $(K_d/n)'$ compared to its optical antipode, which causes the observed isomer concentration dependence of the stereospecificity.

3.5. ^{13}C and ^{19}F NMR of the [5-^{13}C] enriched isomers bound to HSA at different mole ratios

Fig. 6 displays the carboxyl/carbonyl region of the ^{13}C NMR spectra at different [5-^{13}C] enriched isomer/HSA mole ratios. With no added isomer (bottom), natural abundance resonances arising from albumin were observed at ~178 and 183–185 ppm [33,34]. When the [5-^{13}C] *R*-isomer/HSA mole ratio was 1/1, two additional ^{13}C resonances (peaks C_α and C_β) were observed at 191.0 and 196.5 ppm. With an increase in the mole ratio to 2/1, these peaks increased equally in intensity relative to the glutamate resonance of the protein at 183–184 ppm [34]. At the mole ratio above 2/1, an additional resonance (peak C_γ) was observed at 195.7 ppm. When an excess amount of the unlabeled *R*-isomer was added in the presence of 2 molar equivalent of the [5-^{13}C] *R*-isomer, the intensities of peaks C_α and C_β were conspicuously decreased with a concomitant appearance of the peak C_γ (data not shown), showing that the binding to the peaks C_α and C_β sites is reversible. From these observations, peaks C_α and C_β should be considered as specific binding while the peak C_γ non-specific binding although the chemical shift of peak C_γ is most probably the weighted average of the shifts in the non-specifically bound (and free) states. Thus, NMR differentiated the two high affinity sites with apparently similar affinities for the *R*-isomer, which were also suggested by the fluorescent probe displacement and the HPFA data. In contrast, the [5-^{13}C] *S*-isomer exhibited a single resonance (peak C_δ) at 195.4 ppm and its line width was narrower than those of the bound *R*-isomer up to a 2/1 mole ratio. When the *S*-isomer/HSA mole ratio was further

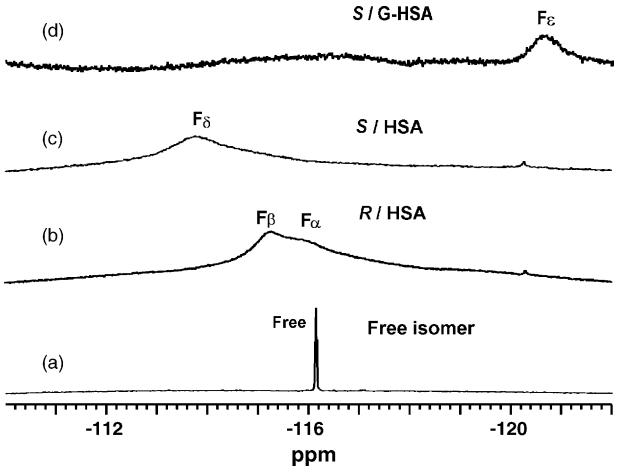

Fig. 7 – ^{19}F NMR spectra of the *R*- or *S*-isomer in either the absence or presence of HSA or G-HSA (2/1 mole ratio of the isomer/HSA or G-HSA complex) at pH 7.4 and 25 °C. The ^{19}F-signal of the free isomer exhibits the splitting pattern due to ^{19}F–^{1}H multiple couplings.

increased above 2/1, the basal portion of peak C_δ became broader, presumably due to the appearance of a non-specific peak (C_γ) around 196 ppm. Thus, two specific binding environments were not evident in the HSA–*S*-isomer complex, suggesting smaller differences in binding modes for the succinimide of the *S*-isomer molecules bound to sites I and II.

^{19}F NMR measurements were also performed at 2/1 mole ratio of the isomer/HSA in order to obtain information about the environment of the 4-bromo-2-fluorobenzyl group of the isomers in the complex. As shown in Fig. 7(b), the two signals for the bound *R*-isomer were observed at −115.9 and −115.4 ppm (designated peaks F_α and F_β, respectively), indicating that the pendent benzyl ring exists in two different environments in the complex with HSA. On the other hand, only one signal (−114.0 ppm, peak F_δ) was observed for the bound *S*-isomer (Fig. 7(c)). These findings corresponded well to those of the ^{13}C NMR measurements.

3.6. *pH and temperature dependence of the isomers specific binding to HSA*

To characterize the protonation state of the succinimide, the pH dependence of the chemical shift of the [5-^{13}C] isomers was examined. Fig. 8(a) shows a pH titration curve for the 5-carbonyl resonance of the [5-^{13}C] isomers collected between pH 3.6 and 8.3 in the absence of HSA. Although broadening of the signal was observed at around pH 5.3–6.4 (data not shown), the pH dependence exhibited a sigmoidal titration curve and was fitted to Eq. (6), which gave the following values: δ_{low} of 197.24 ± 0.04 ppm, δ_{high} of 178.99 ± 0.05 ppm, and p*K* of 5.81 ± 0.01. Since the succinimide is the only dissociable group in the isomers, this pK value corresponds to its ionization state and thus reflects that the isomers are negatively charged at physiological pH values.

Fig. 8(b) illustrates the effects of pH on the isomers specific binding to HSA acquired at 2/1 mole ratio of the isomer/HSA.

Table 3 – Dissociation constants for the isomers binding to HSA in the pH range of 5.0–9.0 at 25 °C[a]

pH	K_{dFL} (μM)	
	R-isomer	S-isomer
5.0	5.4 ± 1.6	17.4 ± 2.2
5.8	3.9 ± 0.6	12.3 ± 1.8
6.4	2.7 ± 0.2	8.2 ± 0.9
7.4	1.7 ± 0.2	7.1 ± 0.6
8.4	1.3 ± 0.1	5.1 ± 0.8
9.0	0.88 ± 0.08	3.7 ± 0.2

[a] 1/15 M phosphate buffers were used.

From the comparison with the ^{13}C chemical shifts of the free isomer at various pHs (Fig. 8(a)), the succinimides corresponding to peaks C_β and C_δ would be almost fully ionized (~96%) in the complexes with HSA, while those corresponding to peak C_α only partially ionized (~66%) (i.e., partially protonated). When the pH of the solution was changed from 7.4 to 6.4, the intensities of peaks for the bound *R*-isomer were reduced with no change in chemical shifts, suggesting that the succinimide rings are solvent-inaccessible and probably involved in electrostatic interactions or hydrogen bonds. As the pH was further decreased to 5.8, these peaks were lost in the noise, but could be restored by back titration with NaOH. The ^{19}F signals of the bound *R*-isomer (F_α and F_β) also exhibited a similar pH-dependent behavior (data not shown). As for the bound *S*-isomer (Fig. 8(b), right), similar pH dependence was obtained, except that a small upfield shift was observed upon a pH change from 7.4 to 6.4 (0.6 ppm, compared with 3.2 ppm for the free form). This finding indicated that the succinimide ring of the *S*-isomer forms electrostatic interactions with HSA, but in contrast to that of the *R*-isomer, is partially exposed to solvent. Since the extreme broadening of the NMR signals hampered the investigation of the interaction with HSA in this pH region, fluorescence quenching was used and the obtained K_{dFL} values at selected pH values are summarized in Table 3. Although pH affected the isomers binding, the finite-and-fixed K_{dFL} values simply indicated that both isomers bind to HSA within this pH range. Therefore, the broadening of the 5-carbonyl resonance near the pK in both HSA–isomer complexes was presumably due to fast proton exchange between the protonated and deprotonated species of the succinimide.

The specific binding of the isomers to HSA was further investigated with regard to temperature. Although the resonance positions and their line widths of the ^{13}C signals of the bound *R*-isomer (peaks C_α and C_β) were independent of the temperature in the range of 5–47 °C (data not shown), the resolution of the ^{19}F signals for the bound *R*-isomer (peaks F_α and F_β) was temperature-dependent. As shown in Fig. 9, peaks F_α and F_β were clearly separated at 8 °C. As the temperature increased, the two peaks moved closer to each other, and above 32 °C they coalesced into a single peak. These results indicated that the system is at equilibrium and the 2-fluorine atom experiences different environments slowly on the ^{19}F NMR time scale at low temperatures but rapidly at high temperatures. A transition from slow to fast exchange on the

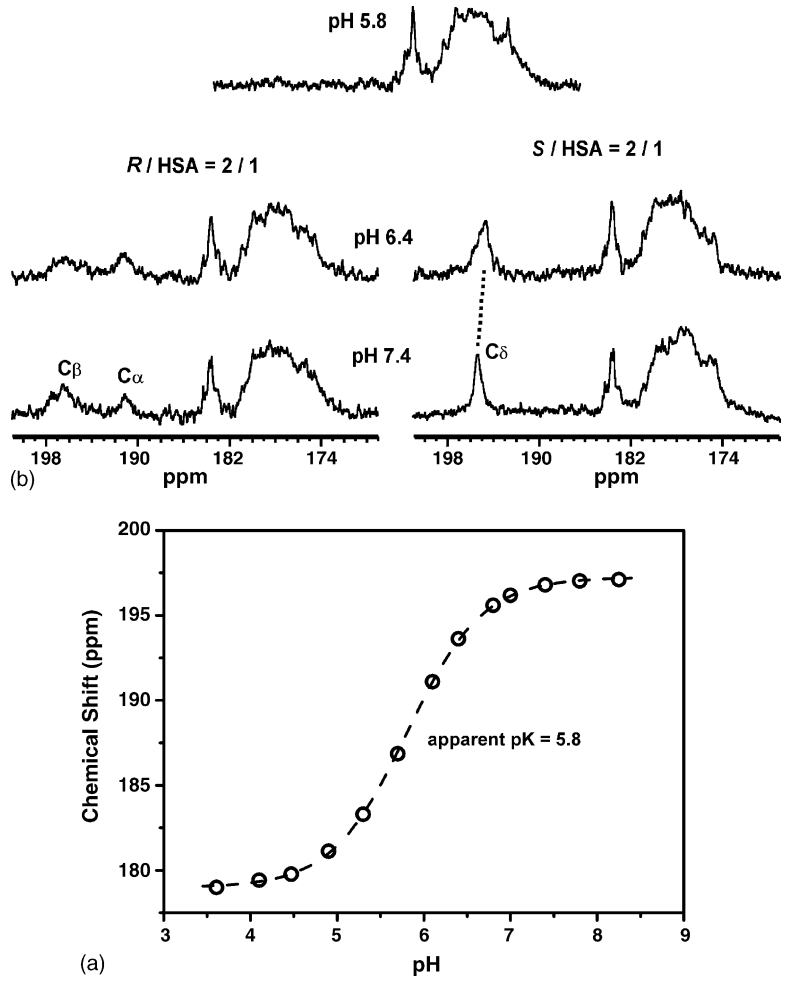

Fig. 8 – (a) pH titration curve of the ^{13}C-enriched 5-carbonyl resonance of the free isomers at 25 °C. (b) ^{13}C NMR spectra (carboxyl/carbonyl region) for a 2/1 mole ratio of the [5-^{13}C] *R*- or *S*-isomer/HSA complex at different pH values. All spectra were determined at 25 °C.

NMR time scale occurs when the exchange rate constant between two states (k_{ex}) = $\pi\Delta\nu/\sqrt{2} = 2.22\Delta\nu$ (where $\Delta\nu$ is the chemical shift difference between the states in s^{-1}) [35]. Since the $\Delta\nu_{19F}$ value between F_α and F_β is 235 s^{-1} (i.e., 0.5 ppm × 470.3 Hz), the k_{ex} value between the *R*-isomer molecules bound to the two specific binding sites was estimated to be approximately 450–600 s^{-1}. On the other hand, the $\Delta\nu_{13C}$ value between peaks C_α and C_β is 690 s^{-1} (i.e., 5.5 ppm × 125.7 MHz), and therefore the *R*-isomer binds to these two sites in slow exchange on ^{13}C NMR time scale because this k_{ex} value (450–600 s^{-1}) is much smaller than the $2.22\Delta\nu_{13C}$ value. In contrast, no temperature dependence was observed for the ^{13}C and ^{19}F NMR signals of the bound *S*-isomer (data not shown), indicating that this isomer is in fast exchange or in very similar magnetic environments between the binding states. The temperature dependence of the binding parameters for the specific binding to HSA was also investigated by means of HPFA. Fig. 10 provides the van't Hoff plots ($-\ln K_{d1}/n_1$ versus $1/T$) for the specific binding, which were essentially linear in the range 15–37 °C. These linear behaviors assumed the heat capacity changes of these binding equilibria to be nearly zero, confirming that the determination of the enthalpy and entropy changes using Eq. (5) was appropriate. From the plots were calculated the three thermodynamic quantities, namely the standard Gibbs energy change (ΔG°), the enthalpy change (ΔH°), and the standard entropy change (ΔS°), which are listed in Table 4.

3.7. *Influence of free fatty acid and glycation on the isomers binding to HSA*

Table 2 also summarizes the binding parameters of the isomers to FA-HSA and G-HSA examined by means of HPFA.

Table 4 – Thermodynamic parameters for the isomers specific binding to HSA at pH 7.4 and 37 °C[a]

Ligand	ΔG° (kJ/mol)	ΔH° (kJ/mol)	ΔS° (J/mol°)
R-isomer	−35.3 ± 0.1	−24.7 ± 1.5	34.1 ± 5.1
S-isomer	−31.6 ± 0.1	−10.8 ± 1.3	67.4 ± 4.4

[a] The standard Gibbs energy change (ΔG°), the enthalpy change (ΔH°), and the standard entropy change (ΔS°) were calculated according to Eq. (5).

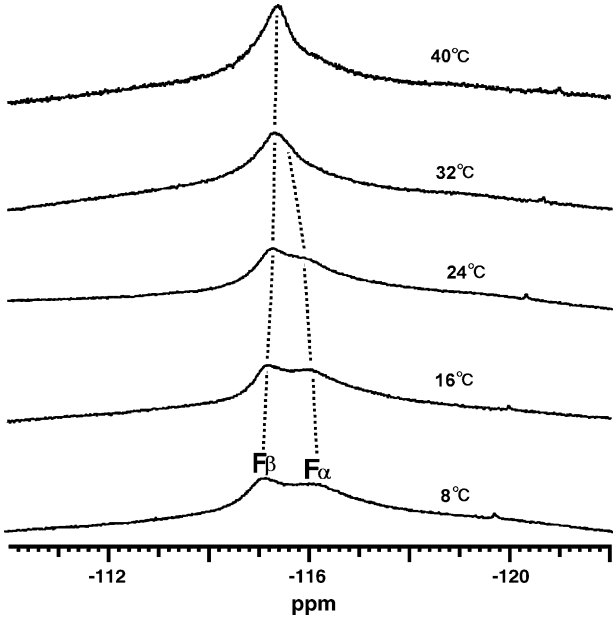

Fig. 9 – ^{19}F NMR spectra for a 2/1 mole ratio of the *R*-isomer/HSA complex at different temperatures in the range of 8–40 °C at pH 7.4.

As for FA-HSA binding, the n_1 values of the *R*- and *S*-isomers were reduced to about 40 and 70%, respectively, as compared with the corresponding values for HSA binding, and the K_{d1} value of the *R*-isomer increased 3.7-fold while that of the *S*-isomer 2.4-fold, reducing the stereospecificity in the specific binding toward the isomers (K_{d1}/n_1 ratio (*S*/*R*)) to one-third that of HSA (from 5.2- to 1.8-fold). On the other hand, the stereospecificity in the non-specific binding almost disappeared (i.e., the $(K_d/n)'$ ratio (*S*/*R*) was almost unity). However, since FA-HSA used in the present study contains as many as 8.1 mole fatty acid per mole albumin (see Section 2.1), the preferential effect of fatty acids on the isomers binding

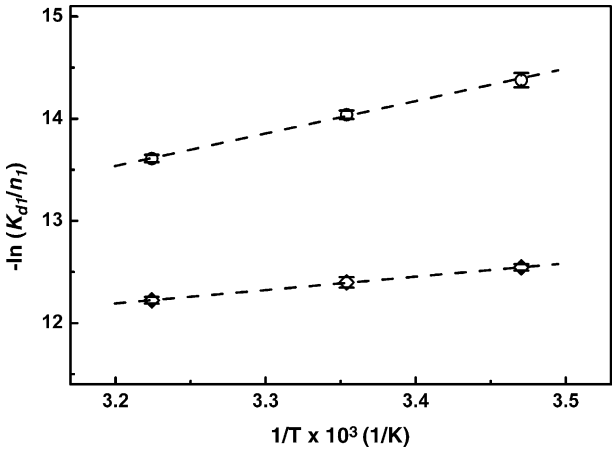

Fig. 10 – Temperature dependence of the K_{d1}/n_1 values (van't Hoff plot) for the interactions of the *R*-isomer (○) and the *S*-isomer (◇) with HSA obtained from HPFA at pH 7.4.

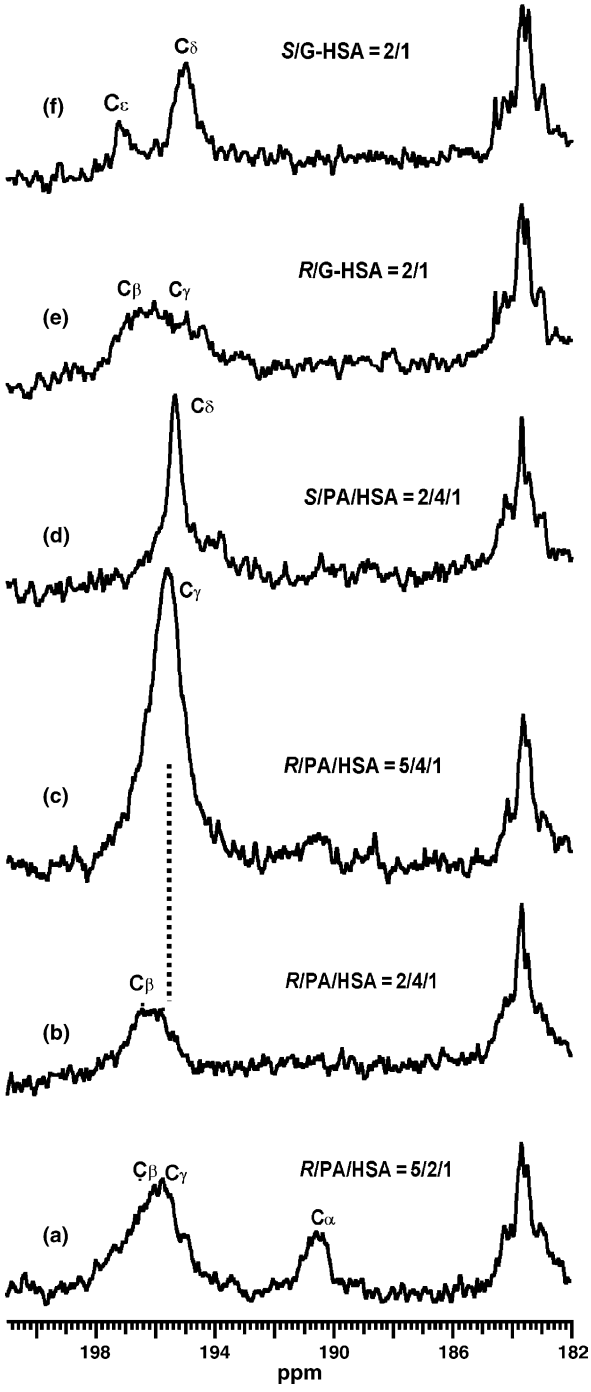

Fig. 11 – Influence of palmitic acid (a–d) and glycation (e and f) on the ^{13}C NMR signals of the bound isomers at different mole ratios at pH 7.4 and 25 °C. PA: palmitic acid.

remains to be investigated. Fig. 11 shows the influence of palmitic acid (PA), a quantitatively and physiologically important saturated fatty acid, on the ^{13}C NMR signals of the specifically bound isomers. When the *R*-isomer was added to the sample at a 2/1 mole ratio of the PA/HSA up to 5 molar equivalents, a similar ^{13}C NMR spectrum (Fig. 11(a)) was observed with the spectral analysis in the absence of PA

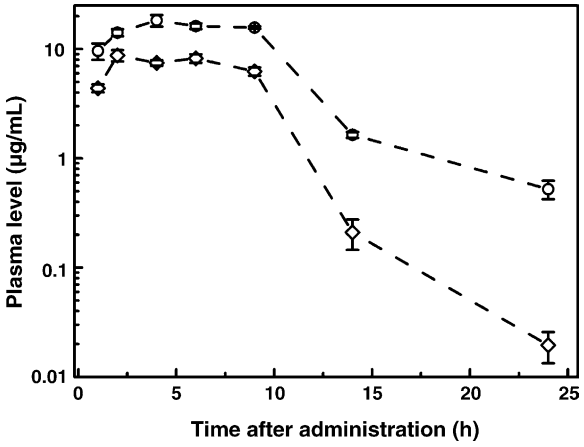

Fig. 12 – Mean plasma levels of the *R*-isomer (○) and the *S*-isomer (◇) in male Wistar rats after single oral administration of 10 mg/kg of the separate isomers. Each point represents the mean ± standard error for three rats.

(Fig. 6). However, when the *R*-isomer was added in the presence of 4 molar equivalents of PA, peak C_α was not observed and the non-specific peak C_γ appeared concomitantly with increases in the *R*-isomer/HSA ratio to 5/1 (Fig. 12(b and c)). In contrast, PA binding had virtually no chemical shift but noticeable line sharpening effect on the ^{13}C resonance (C_δ) of the *S*-isomer bound to HSA (Fig. 11(d)), suggesting little change in the magnetic environment but a significant increase in free form or in motional behavior around its succinimide ring.

As for G-HSA binding, the n_1 value of the *R*-isomer was significantly reduced, and its K_{d1} value increased 2.5-fold whereas that of the *S*-isomer was not appreciably altered (Table 2). As a consequence, the stereospecificity in the specific binding was reduced to 1.7-fold. However, the non-specific binding of the isomers was little affected, which concurs with the data reported previously [36]. In the ^{13}C NMR spectrum for a 2/1 mole ratio of the [5-^{13}C] *R*-isomer/G-HSA (Fig. 11(e)), a single unresolved peak (peaks C_β and C_γ) was observed but peak C_α was not, thus indicating that the *R*-isomer binding to the peak C_α site is also inhibited. In contrast, when the *S*-isomer was added to the G-HSA solution, an additional small and narrow resonance (peak C_ε) was observed at 197.2 ppm (Fig. 11(f)). Comparison of this chemical shift value with those of the free isomer observed in the pH titration curve (Fig. 8(a)) suggests that the succinimide bound to the peak C_ε site is almost completely ionized (~100%). Influence of PA binding and glycation on the isomers binding was also characterized by ^{19}F NMR. These perturbations selectively inhibited the *R*-isomer binding to the peak F_α site (data not shown). In contrast, although PA binding had little effect on the ^{19}F NMR spectrum of the *S*-isomer bound to HSA (not shown), that of the G-HSA–*S*-isomer complex showed the absence of peak F_δ and the appearance of peak F_ε (Fig. 7(d)) 4.5 ppm upfield from the free isomer peak (Fig. 7(a)). This large upfield shift is interpreted as due to a substantial contribution from ring current effect [37]. Moreover, these NMR observations allow the signal assignment of the isomers interacting with sites I and II. Since site II (subdomain IIIA binding cavity) is the second favorable sites for fatty acids [13,38] and close to the primary glycation site Lys525 in subdomain IIIB [5,39], drug binding to site II is often inhibited by relatively higher concentrations of long-chain fatty acids [40,41] or by HSA glycation [2,4,5]. Therefore, comparison of the HSA–*R*-isomer complex with that in the presence of PA or glycation allows the assignment of peak C_α to the *R*-isomer bound to site II and peak C_β to that bound to site I, respectively. Likewise, peak F_α should be assigned to the *R*-isomer bound to the site II and peak F_β to that bound to the site I.

4. Discussion

Despite its susceptibility to hydrolysis in aqueous solution, the *R*-isomer has a highly potent and long-lasting AKR1B inhibitory effect [6]. A possible reason for this promising profile should be its stereospecific interaction with the target enzyme AKR1B [9]. Another may be associated with the plasma protein binding of this compound. The aim of the present study was to investigate the interaction with plasma proteins, particularly with HSA. Because of the conformational flexibility and the allosteric interactions between multiple binding sites, static structural analysis may not sufficiently reveal the structure–function relations influencing drug–HSA interactions. The present comparative study of binding characteristics of the *R*-isomer and its optical antipode (*S*-isomer), using several techniques in a concerted fashion, allowed us to decipher the exact nature of the HSA–*R*-isomer interaction; this will provide a basis for systematically considering its plasma protein binding as a factor in pharmacokinetics and pharmacodynamics.

4.1. *Binding characteristics of the R- and S-isomers to plasma proteins*

Fluorescence quenching studies showed that HSA binds the *R*-isomer more than seven-fold stronger than α_1-AGP (Table 1). This finding indicates that HSA is the major binding protein in human plasma, because HSA normally comprises 60% of total plasma protein [11]. The results of HPFA and NMR clearly revealed that both isomers bind to two specific sites on HSA, which were further found to be sites I and II using fluorescent probes and a marker drug warfarin. These two primary binding sites had very similar dissociation constants for each of the isomers, but exhibited distinct stereospecificity toward the isomers. The obtained dissociation constants of the *R*-isomer and stereospecificity (*S*/*R*) ratios for the specific binding were in good agreement, within the experimental error, for each of the fluorescence quenching, kinetic (hydrolysis), and HPFA methods (Tables 1 and 2); these were, respectively, 1.6–2.1 μM and 4.2–5.2.

Although specific and non-specific binding sites on HSA exhibited opposite stereospecific discrimination (Fig. 5(a)), the interaction at the specific binding sites (sites I and II) is clinically important, because the therapeutic concentrations of the *R*-isomer (<2 μM) are much lower than the physiological concentration of HSA (~600 μM) [8]. The calculated binding ratio of the *R*-isomer to HSA was significantly higher (99.8–

99.9%) than that of the S-isomer (99.3–99.5%),[2] indicating that the free fraction of the R-isomer is several fold smaller than that of the S-isomer. Also the k_{app} determined at 600 μM of HSA, using Eq. (3) with K_{dapp}, k_b and k_f values in Table 1, was found to be $2.8 \times 10^{-3}\ h^{-1}$ for the R-isomer and $5.2 \times 10^{-3}\ h^{-1}$ for the S-isomer. Thus, differences in the binding affinity and the hydrolysis rate of the bound form would reflect the disparity in actual hydrolysis rates in HSA solution between the isomers, and the hydrolytic inactivation of the R-isomer will be considerably (up to 40-fold) retarded relative to the free isomer.

Several studies have shown that the binding of drugs to both sites I and II is pH dependent over the pH range 6–9, due to a conformational change of HSA, the so-called neutral to base or N–B transition [42–44]. Although the NMR analysis during the N–B transition was hampered by the extreme broadening of the NMR signals of the bound isomers near the pK of 5.8 (Fig. 8(b)), the pH dependence of K_{dFL} (Table 3) showed that the N–B transition is also involved in the pH dependent binding of the isomers, and the B form of HSA has more affinity with the isomers than the N form. However, there appears to be a larger pH dependence of the R-isomer affinity (Table 3). Moreover, on the other hand, a smaller pH dependence of the ^{13}C NMR signals of the bound R-isomer (Fig. 8(b)) and a smaller value of k_b in hydrolysis retardation with HSA (Table 1) showed that the succinimide ring of the R-isomer is more buried or shielded in the HSA molecule. From the small influence of surface or solvent-exposed electrostatic interactions on protein stability [45,46], the partial exposure of the succinimide ring of the S-isomer to the solvent implies that the HSA–S-isomer complex is less stable than the HSA–R-isomer complex. These results, together with a substantially lower affinity of compound 1 for HSA, strongly suggest that the negatively charged succinimide ring, especially in the R configuration, is important for both the stronger binding to HSA and the stabilization against the hydrolysis.

[2] The free concentrations of the isomers were calculated, using Eq. (4) with a single class of specific binding (z = 1) and non-specific binding.

$$r = \frac{L_b}{P_t} = \frac{n_1 L_f}{K_{d1} + L_f} + \frac{L_f}{(K_d/n)'}$$

The total ligand concentration (L_t) can be expressed as:

$$L_t = L_f + L_b = L_f + \frac{n_1 L_f P_t}{K_{d1} + L_f} + \frac{L_f P_t}{(K_d/n)'}$$

From this equation, the following quadratic equation can be derived.

$$\left\{1 + \frac{P_t}{(K_d/n)'}\right\} L_f^2 + \left\{K_{d1} - L_t + n_1 P_t + \frac{P_t K_{d1}}{(K_d/n)'}\right\} L_f - L_t K_{d1} = 0$$

Then, the free isomer concentration (L_f) is given by:

$$L_f = \frac{\sqrt{\left\{K_{d1} - L_t + n_1 P_t + \frac{P_t K_{d1}}{(K_d/n)'2}\right\} + 4\left\{1 + \frac{P_t}{(K_d/n)'}\right\} L_t K_{d1}} - \left\{K_{d1} - L_t + n_1 P_t + \frac{P_t K_{d1}}{(K_d/n)'}\right\}}{2\{1 + P_t/(K_d/n)'\}}$$

The L_f value was calculated at P_t (600 μM) and a fixed total concentration of L_t (< 10 μM), using the obtained values for n_1, K_{d1} and $(K_d/n)'$ at 15, 25 and 37 °C. Under these conditions the estimated binding ratios (L_b/L_t) or free fractions (L_f/L_t) of the isomers were almost constant, and these values were extracted. The same procedure was used to estimate the binding ratios (L_b/L_t) or free fractions (L_f/L_t) of the isomers to FA-HSA or G-HSA. The calculated binding ratios to HSA, FA-HSA and G-HSA at 37 °C were 99.8, 98.8–98.9 and 99.4–99.5, respectively. These calculated ratios were close to that in human serum (99.2–99.4%) (unpublished data).

4.2. Stereospecific binding modes of the isomers to HSA

Protein–ligand interaction usually undergoes hydrophobic association (step 1) and subsequent other intermolecular interactions (step 2) [47]. In step 1, the release of restricted water molecules from the interacting hydrophobic surface generates a considerable positive ΔS°. In step 2, hydrogen bonds and van der Waals interactions contribute to negative ΔH° and ΔS° because these formations are exothermic, and will be accompanied by a decrease in the translational–rotational mobility, while electrostatic interactions to positive ΔS° by releasing hydration water molecules around the charged species to the bulk solvent. In the present study, ΔS° for both isomers specific binding was positive (Table 4), suggesting that hydrophobic interactions play an important role in the complexes formation and the conformational entropy losses may be relatively small, partly due to the rigidity of the isomers. This observation is in marked contrast to the interaction between the R-isomer and the target enzyme AKR1B characterized by predominantly large negative ΔH° [9]. However, it should be noted that ΔH° and ΔS° for the HSA–R-isomer formation are more negative than those for the HSA–S-isomer formation. These differences may suggest that hydrogen bonds also contribute to the R-isomer binding to HSA, while electrostatic interactions to the S-isomer complex.

Further insight into important interactions responsible for this stereospecific binding was obtained by the assigned NMR signals of the bound isomers and their ionization states, with the aid of the crystal structure of HSA [5,11,48]. Since the succinimide ring of the isomer is mostly deprotonated (negatively charged) at physiological pH values (Fig. 8(a)), it can form an electrostatic interaction with a positively charged residue, or a charged hydrogen bond with a hydrogen bond donor upon complexation. When the succinimide ring of the isomer forms an electrostatic interaction, it would be also fully deprotonated on the basis of the chemical shift of the 5-^{13}C labeled succinimide ring, whereas if the bound isomer forms a hydrogen bond with a hydrogen bond donor, the succinimide of the isomer molecules becomes partially protonated. In the present case, since the R- and S-isomers that are bound to site I (peaks C_β and C_δ, respectively) are almost fully ionized based on their chemical shifts, they are likely to bind to an electrostatic focal point (Lys199, Arg218 and His242) in subdomain IIA (site I). In the subdomain IIIA (site II), on the other hand, the negatively charged S-isomer (peak C_δ) may also interact electrostatically with a positive center Arg410, whereas the partially protonated R-isomer (peak C_α) could be hydrogen bonded to unionized and hydrogen bond donor residues such as Tyr411 and Ser489 forming this site together with Arg410. These binding modes are in agreement with the binding natures inferred from the thermodynamic analysis. In addition, the assumed site II-oriented perturbations such as

Table 5 – Plasma and tissue levels of the *R*- or *S*-isomer at 4 h and 3 day after repeated oral administration of 0.6 mg/kg/day of the separate isomers for 5 day in rats ($n = 3$)[a]

Biological matrix	R-isomer		S-isomer	
	4 h	3 d	4 h	3 d
Plasma	807 ± 52	22.9 ± 1.7	631 ± 45	6.1 ± 0.9
Kidney	1.72 ± 0.08	0.35 ± 0.02	0.41 ± 0.03	<0.01
Sciatic nerve	0.83 ± 0.05	0.42 ± 0.03	0.05 ± 0.01	<0.01
Lens	0.10 ± 0.02	0.14 ± 0.02	n.d.[b]	n.d.

[a] Male Wistar rats were used. Each level represents the mean ± standard error (ng/mL) and the mean ± standard error (ng/mg) for plasma and wet tissues, respectively.
[b] n.d.: not detected.

fatty acid binding or glycation reduced the stereospecificity ratio to one-third of that for HSA, probably due to preferential inhibition of the *R*-isomer binding to site II (Table 2). Taken together, these results strongly suggested that the difference in the binding mode at site II might be regarded as a major cause of stereospecificity. Another corroborating finding is that the stereospecificity ratio observed in RSA is comparable to that observed in HSA. Since the amino acid sequences and resulting binding chemistries of the IIIA pockets are conserved to a much greater degree between these two species [11], this observation is pertinent to the above interpretation. In the G-HSA–*S*-isomer complex, on the other hand, the n_1 value of 1.5 (Table 2) and the appearance of peak C_ε (Fig. 11(f)) indicated that the *S*-isomer might be still bound within site II with a different binding mode. The upfield shift of the 2-fluorine signal in the ^{19}F NMR spectrum (Fig. 7(d)) invokes a stacking interaction of the 4-bromo-2-fluorobenzyl group with a nearby aromatic ring important for site II ligands binding, perhaps Tyr411 [49] or Phe488.

4.3. *Estimation of the R-isomer binding characteristics in diabetic plasma*

Free fatty acid and non-enzymatic glycation levels were found to be significantly elevated in diabetic patients [50–53]. Since these pathophysiological perturbations often decrease the binding of various drugs to HSA [1–5], the binding characteristics of the isomers were examined using FA-HSA and G-HSA as typical models of HSA present in diabetic plasma. Specific and non-specific binding parameters for both isomers were significantly changed in FA-HSA, compared to those in HSA (Table 2). This result correlates with the X-ray data that saturation of fatty acid sites causes a marked conformational change of HSA [13]. However, based on the binding parameters, the binding ratio of the *R*-isomer to FA-HSA is predicted to slightly decrease at most 1% at therapeutic concentrations (see footnote 2). Also, that of the *R*-isomer to G-HSA was estimated to be virtually unaltered (0.4% decrease), despite significant changes in the specific binding parameters (n_1 and K_{d1}). Thus, the fact that the *R*-isomer can bind to more than one site on HSA should reduce the effects of fatty acid binding and glycation on the degree of its binding to HSA. Moreover, since elevated fatty acids or non-enzymatic glycation in diabetic plasma comprise a relatively small proportion of total albumin [1,51,53], the significance of these perturbations should be minor with respect to the binding to HSA in clinical practice. Also from these HSA-binding characteristics, it seems unlikely that the *R*-isomer will participate in drug–drug interactions related to binding to HSA in diabetic patients because fewer drugs would essentially compete with the tightly bound *R*-isomer (dissociation constants in the low μM range) and the *R*-isomer in lower therapeutic plasma range in turn may not affect the bindings of other drugs to HSA.

4.4. *Physiological and clinical significance of the binding to serum albumin*

Although the isomers are only slightly soluble in aqueous solution at physiological pH, the strong and reversible binding to more than one site on HSA increases their solubility (up to mM). The binding ratios of the isomers to HSA are high, as already mentioned, and are similar to those of circulating fatty acids [5,54]. However, the exchange rate between sites I and II obtained by ^{19}F NMR analysis (450–600 s^{-1}) is much faster than the desorption rate of long-chain fatty acids from albumin (<10 s^{-1}) [34,55], but rather comparable to the rate of medium-chain fatty acids desorption (>115 s^{-1}) [56]. Since the latter fatty acids are rapidly absorbed even in patients with impaired absorption of the former fatty acids [57], we also examined preliminary distribution profiles of the isomers in rats. Fig. 12 shows the mean plasma levels after single oral administration of the separate isomers. As is the case for most chiral drugs with a passive absorption process [58], the absorption profiles of the isomers were similar to each other with a mean T_{max} of 4 h, but the *S*-isomer level was lower than the *R*-isomer level. This may be because the *S*-isomer can be distributed more rapidly to tissues due to its significantly weaker binding to RSA (Table 1). Table 5 lists the mean levels in target tissues susceptible to diabetic complications as well as in plasma at around the peak plasma concentration time (4 h) and the terminal phase (3 d) after repeated oral administration. Both isomers seemed to be relatively favorably transported from the bloodstream into the target tissues with low blood flow such as sciatic nerve and lens. Substantial stereospecific differences with respect to the residence time in these tissues probably reflect differences in AKR1B stereospecificity toward the isomers [9], based on almost complete conservation in active site residues between the rat and human enzyme [59]. These data were consistent with the fact that the *R*-isomer is much more potent than the *S*-isomer on the basis of the abilities to inhibit sorbitol accumulation in the sciatic nerve of diabetic rats [6].

From these results and from similar affinities and stereospecificities for the isomers between HSA and RSA (Table 1),

the *R*-isomer can be expected to be well transferred to the tissues and to produce long-lasting AKR1B inhibition in the target tissues of humans. Recent clinical trials have revealed that the *R*-isomer penetrates the sural nerve and inhibits sorbitol accumulation in patients with DSP [8], but the compound 1 (hydrolysis product) level in human plasma is slightly greater than would be expected from its level in rat plasma (unpublished data). The latter finding may be explained by subtle but significant interspecies differences in dissociation constant and hydrolysis rate of the bound *R*-isomer between HSA and RSA (Table 1). Thus, a stable complex between the *R*-isomer and serum albumin contributes, at least partly, to the favorable pharmacological properties by circulating in the body for a long time and by efficiently passing the isomer into the target tissues. Further studies are needed to fully evaluate the biological and therapeutic significance of these findings.

In summary, this study has characterized the interaction of a potent spirosuccinimide type aldose reductase (AKR1B) inhibitor, AS-3201 (*R*-isomer), with HSA, in comparison with that of the optical antipode (*S*-isomer). The *R*-isomer was reversibly and more strongly bound to specific binding sites I and II on HSA, and this complex formation significantly retarded the hydrolysis of the *R*-isomer at physiological pH levels. Putative binding modes for the isomers, considered from direct NMR observations and van't Hoff analysis of the specific binding with the aid of the crystal structure of HSA, indicated that the difference in the interaction mode at site II between the isomers might be a major cause of stereospecificity. Preliminary absorption and distribution profiles of the *R*-isomer also suggested that the stable HSA–*R*-isomer complex contributes to the favorable oral bioavailability as well as to the long-lasting pharmacological effect. These characteristics, together with the small effect of free fatty acid and glycation on the *R*-isomer binding ratio, may be helpful to better understand both the relationship between pharmacokinetic and pharmacodynamic properties of this compound and its therapeutic relevance in the treatment of diabetic complications.

Acknowledgements

The authors are grateful to Mr. A. Itogawa for carrying out some ^{13}C NMR measurements, to Mr. Y. Ono for the preparation of the biological samples, and to Mr. G. Argyle for reading the manuscript. They also thank Dr. K. Chiba, the director of this laboratory, for his continual support and encouragement.

REFERENCES

[1] Mereish KA, Rosenberg H, Cobby J. Glucosylated albumin and its influence on salicylate binding. J Pharm Sci 1982;71:235–8.
[2] Ruiz-Cabello F, Erill S. Abnormal serum protein binding of acidic drugs in diabetes mellitus. Clin Pharmacol Ther 1984;36:691–5.
[3] Tsuchiya S, Sakurai T, Sekiguchi S. Nonenzymatic glucosylation of human serum albumin and its influence on binding capacity of sulfonylureas. Biochem Pharmacol 1984;33:2967–71.
[4] McNamara PJ, Blouin RA, Brazzell RK. The protein binding of phenytoin, propranolol, diazepam, and AL01576 (an aldose reductase inhibitor) in human and rat diabetic serum. Pharm Res 1988;5:261–5.
[5] Peters Jr T. Ligand Binding by Albumin. In All about Albumin. In: Biochemistry Genetics and Medical Applications. San Diego: Academic Press, 1996. p. 76–132.
[6] Negoro T, Murata M, Ueda S, Fujitani B, Ono Y, Kuromiya A, et al. Novel, highly potent aldose reductase inhibitors: (*R*)-(−)-2-(4-bromo-2-fluorobenzyl)-1,2,3,4-tetrahydropyrrolo[1,2-a]pyrazine-4-spiro-3'-pyrrolidine-1,2′,3 5′-tetrone (AS-3201) and its congeners. J Med Chem 1998;41:4118–29.
[7] Yabe-Nishimura C. Aldose reductase in glucose toxicity: a potential target for the prevention of diabetic complications. Pharmacol Rev 1998;50:21–33.
[8] Bril V, Buchanan RA. Aldose reductase inhibition by AS-3201 in sural nerve from patients with diabetic sensorimotor polyneuropathy. Diabetes Care 2004;27:2369–75.
[9] Kurono M, Fujiwara I, Yoshida K. Stereospecific interaction of a novel spirosuccinimide type aldose reductase inhibitor, AS-3201, with aldose reductase. Biochemistry 2001; 40:8216–26.
[10] Hargreaves MK, Pritchard JG, Dave HR. Cyclic carboxylic monoimides. Chem Rev 1970;70:439–69.
[11] Carter DC, Ho JX. Structure of serum albumin. Adv Protein Chem 1994;45:153–203.
[12] Curry S, Mandelkow H, Brick P, Franks N. Crystal structure of human serum albumin complexed with fatty acid reveals an asymmetric distribution of binding sites. Nat Struct Biol 1998;5:827–35.
[13] Bhattacharya AA, Grune T, Curry S. Crystallographic analysis reveals common modes of binding of medium and long-chain fatty acids to human serum albumin. J Mol Biol 2000;303:721–32.
[14] Sudlow G, Birkett DJ, Wade DN. The characterization of two specific drug binding sites on human serum albumin. Mol Pharmacol 1975;11:824–32.
[15] He XM, Carter DC. Atomic structure and chemistry of human serum albumin. Nature 1992;358:209–15.
[16] Birkett DJ, Myers SP, Sudlow G. The fatty acid content and drug binding characteristics of commercial albumin preparations. Clin Chim Acta 1978;85:253–8.
[17] Mizuno K, Toyosato M, Yabumoto S, Tanimizu I, Hirakawa H. A new enzymatic method for colorimetric determination of free fatty acids. Anal Biochem 1980;108:6–10.
[18] Sudlow G, Birkett DJ, Wade DN. Further characterization of specific drug binding sites on human serum albumin. Mol Pharmacol 1976;12:1052–61.
[19] Liu R, Sharom FJ. Site-directed fluorescence labeling of P-glycoprotein on cysteine residues in the nucleotide binding domains. Biochemistry 1996;35:11865–73.
[20] Eftink MR. Fluorescence methods for studying equilibrium macromolecule-ligand interactions. Methods Enzymol 1997;278:221–57.
[21] Connors KA, Mollica Jr JA. Theoretical analysis of comparative studies of complex formation. J Pharm Sci 1966;55:772–80.
[22] Shibukawa A, Nagao M, Kuroda Y, Nakagawa T. Stereoselective determination of free warfarin concentration in protein binding equilibrium using direct sample injection and an on-line liquid chromatographic system. Anal Chem 1990;62:712–6.
[23] Shibukawa A, Kuroda Y, Nakagawa T. High-performance frontal analysis for drug-protein binding study. J Pharm Biomed Anal 1999;18:1047–55.

[24] Pinkerton TC. High-performance liquid chromatography packing materials for the analysis of small molecules in biological matrices by direct injection. J Chromatogr 1991;544:13–23.
[25] Bevington PR, Robinson DK. Data Reduction and Error Analysis for the Physical Sciences. New York: McGraw-Hill, 1992.
[26] Cleland WW. Statistical analysis of enzyme kinetic data. Methods Enzymol 1979;63:500–13.
[27] Peters Jr T. Serum albumin. Adv Protein Chem 1985;37: 161–245.
[28] Smith EL, Brown DM, Weimer HE, Winzler RJ. Sedimentation, diffusion, and molecular weight of a mucoprotein from human plasma. J Biol Chem 1950;185:569–75.
[29] Chignell CF. Optical studies of drug-protein complexes II. Interaction of phenylbutazone and its analogues with human serum albumin. Mol Pharmacol 1969;5:244–52.
[30] Muller N, Lapicque F, Drelon E, Netter P. Binding sites of fluorescent probes on human serum albumin. J Pharm Pharmacol 1994;46:300–4.
[31] Malamas MS, Hohman TC, Millen J. Novel spirosuccinimide aldose reductase inhibitors derived from isoquinoline-1,3-diones: 2-[(4-bromo-2-fluorophenyl)methyl]-6-fluorospiro[isoquinoline-4(1H),3'-pyrrol idine]-1,2',3 5'(2H)-tetrone and congeners. 1. J Med Chem 1994;37:2043–58.
[32] Reist M, Carrupt PA, Francotte E, Testa B. Chiral inversion and hydrolysis of thalidomide: mechanisms and catalysis by bases and serum albumin, and chiral stability of teratogenic metabolites. Chem Res Toxicol 1998;11:1521–8.
[33] Cistola DP, Small DM, Hamilton JA. Carbon 13 NMR studies of saturated fatty acids bound to bovine serum albumin I. The filling of individual fatty acid binding sites. J Biol Chem 1987;262:10971–9.
[34] Cistola DP, Small DM. Fatty acid distribution in systems modeling the normal and diabetic human circulation A 13C nuclear magnetic resonance study. J Clin Invest 1991;87:1431–41.
[35] Sandstrom J. Dynamic NMR Spectroscopy.. London: Academic Press, 1982.
[36] Koyama H, Sugioka N, Uno A, Mori S, Nakajima K. Effects of glycosylation of hypoglycaemic drug binding to serum albumin. Biopharm Drug Dispos 1997;18:791–801.
[37] Gregory DH, Gerig JT. Prediction of fluorine chemical shifts in proteins. Biopolymers 1991;31:845–58.
[38] Curry S, Brick P, Franks NP. Fatty acid binding to human serum albumin: new insights from crystallographic studies. Biochim Biophys Acta 1999;1441:131–40.
[39] Zoellner H, Hou JY, Hochgrebe T, Poljak A, Duncan MW, Golding J, et al. Fluorometric and mass spectrometric analysis of nonenzymatic glycosylated albumin. Biochem Biophys Res Commun 2001;284:83–9.
[40] Bohney JP, Feldhoff RC. Effects of nonenzymatic glycosylation and fatty acids on tryptophan binding to human serum albumin. Biochem Pharmacol 1992;43:1829–34.
[41] Chuang VT, Otagiri M. How do fatty acids cause allosteric binding of drugs to human serum albumin? Pharm Res 2002;19:1458–64.
[42] Peters Jr T. The Albumin Molecule: Its Structure and Chemical Properties. In All about Albumin: Biochemistry. In: Genetics and Medical Applications.. San Diego: Academic Press, 1996. 9–75.
[43] Wilting J, 't Hart BJ, de Gier JJ. The role of albumin conformation in the binding of diazepam to human serum albumin. Biochim Biophys Acta 1980;626:291–8.
[44] Wilting J, van der Giesen WF, Janssen LHM. Weideman MM, Otagiri M, Perrin JH. The effect of albumin conformation on the binding of warfarin to human serum albumin. The dependence of the binding of warfarin to human serum albumin on the hydrogen, calcium, and chloride ion concentrations as studied by circular dichroism, fluorescence, and equilibrium dialysis. J Biol Chem 1980;255:3032–7.
[45] Sali D, Bycroft M, Fersht AR. Surface electrostatic interactions contribute little to stability of barnase. J Mol Biol 1991;220:779–88.
[46] Sun DP, Sauer U, Nicholson H, Matthews BW. Contributions of engineered surface salt bridges to the stability of T4 lysozyme determined by directed mutagenesis. Biochemistry 1991;30:7142–53.
[47] Ross PD, Subramanian S. Thermodynamics of protein association reactions: forces contributing to stability. Biochemistry 1981;20:3096–102.
[48] Sugio S, Kashima A, Mochizuki S, Noda M, Kobayashi K. Crystal structure of human serum albumin at 2.5 A resolution. Protein Eng 1999;12:439–46.
[49] Watanabe H, Tanase S, Nakajou K, Maruyama T, Kragh-Hansen U, Otagiri M. Role of arg-410 and tyr-411 in human serum albumin for ligand binding and esterase-like activity. Biochem J 2000;349:813–9.
[50] Fraze E, Donner CC, Swislocki AL, Chiou YA, Chen YD, Reaven GM. Ambient plasma free fatty acid concentrations in noninsulin-dependent diabetes mellitus: evidence for insulin resistance. J Clin Endocrinol Metab 1985;61:807–11.
[51] Peters Jr T. Clinical Aspects: Albumin Medicine. In All about Albumin: Biochemistry. In: Genetics and Medical Applications.. San Diego: Academic Press, 1996. 251–84.
[52] Gould BJ, Hall PM, Cook JG. A sensitive method for the measurement of glycosylated plasma proteins using affinity chromatography. Ann Clin Biochem 1984;21:16–21.
[53] Gerich JE, Martin MM, Recant L. Clinical and metabolic characteristics of hyperosmolar nonketotic coma. Diabetes 1971;20:228–38.
[54] Spector AA, Plasma. Albumin as a Lipoprotein. In: Scanu AM, Spector AA, editors. Biochemistry and Biology of Plasma Lipoproteins.. New York: Marcel Dekker; 1986. p. 247–79.
[55] Daniels C, Noy N, Zakim D. Rates of hydration of fatty acids bound to unilamellar vesicles of phosphatidylcholine or to albumin. Biochemistry 1985;24:3286–92.
[56] Kenyon MA, Hamilton JA. ^{13}C NMR studies of the binding of medium-chain fatty acids to human serum albumin. J Lipid Res 1994;35:458–67.
[57] Bach AC, Babayan VK. Medium-chain triglycerides: an update. Am J Clin Nutr 1982;36:950–62.
[58] Jamali F, Mehvar R, Pasutto FM. Enantioselective aspects of drug action and disposition: therapeutic pitfalls. J Pharm Sci 1989;78:695–715.
[59] Jez JM, Bennett MJ, Schlegel BP, Lewis M, Penning TM. Comparative anatomy of the aldo-keto reductase superfamily. Biochem J 1997;54:625–36.